Rapid starch degradation in the wood of olive trees under heat and drought is permitted by three stress-specific beta amylases

Mor Tsamir-Rimon[1,2], Shifra Ben-Dor[3], Ester Feldmesser[3], Yaara Oppenhimer-Shaanan[1], Rakefet David-Schwartz[4], Alon Samach[2] and Tamir Klein[1]

[1]Plant & Environmental Sciences Department, Weizmann Institute of Science, Rehovot 76100, Israel; [2]The Robert H. Smith Institute of Plant Sciences and Genetics in Agriculture, The Robert H. Smith Faculty of Agriculture, Food and Environment, The Hebrew University of Jerusalem, Rehovot 76100, Israel; [3]Life Science Core Facilities, Weizmann Institute of Science, Rehovot 76100, Israel; [4]Institute of Plant Sciences, Agricultural Research Organization, Volcani Center, Rishon LeZion 7505101, Israel

Author for correspondence:
Tamir Klein
Email: tamir.klein@weizmann.ac.il

Received: *10 February 2020*
Accepted: *2 June 2020*

New Phytologist (2021) **229:** 1398–1414
doi: 10.1111/nph.16907

Key words: carbon source, drought response, drought tolerance, mannitol, starch degradation, starch synthesis.

Summary

- Carbon reserve use is a major drought response in trees, enabling tree survival in conditions prohibiting photosynthesis. However, regulation of starch metabolism under drought at the whole-tree scale is still poorly understood.
- To this end, we combined measurements of nonstructural carbohydrates (NSCs), tree physiology and gene expression. The experiment was conducted outside on olive trees in pots under 90 d of seasonal spring to summer warming. Half of the trees were also subjected to limited water conditions for 28 d.
- Photosynthesis decreased in dehydrating trees from 19 to 0.5 μmol m^{-2} s^{-1} during the drought period. Starch degradation and mannitol production were a major drought response, with mannitol increasing to 71% and 41% out of total NSCs in shoots and roots, respectively. We identified the gene family members potentially relevant either to long-term or stress-induced carbon storage. Partitioning of expression patterns among β amylase and starch synthase family members was observed, with three β amylases possibly facilitating the rapid starch degradation under heat and drought.
- Our results suggest a group of stress-related, starch metabolism genes, correlated with NSC fluctuations during drought and recovery. The daily starch metabolism gene expression was different from the stress-mode starch metabolism pattern, where some genes are uniquely expressed during the stress-mode response.

Introduction

Nonstructural carbohydrates (NSCs), largely starch, are major substrates for primary and secondary plant metabolism, including functions in energy metabolism, transport and osmoregulation (Hartmann & Trumbore, 2016). At a whole plant scale, NSC buffers asynchrony of carbon supply and demand, i.e. the temporal decoupling between assimilation, respiration and growth. Plants are autotrophic organisms, however their survival must be ensured even in conditions prohibiting photosynthesis, such as deciduousness. For example, in high latitudes, spring leafout in forests is largely sponsored by starch degradation in deciduous tree branches (Keel *et al*., 2007; Klein *et al.* 2016). In trees, long-term carbon storage is located in parenchyma woody tissues: branch, stem and root (Sauter & van Cleve, 1991; Hartmann & Trumbore, 2016). When a need for carbon arises, starch and other reserves are degraded to soluble sugars, which can be mobilized through the tree in the xylem and inner bark (Bustan *et al*., 2011).

An example for storage depletion following carbon demand is under prolonged drought conditions (Chehab *et al*., 2009; Mitchell *et al*., 2013; Klein *et al*., 2014; Lloret *et al*., 2018). Notably, even under stress conditions, trees maintain a minimum threshold content of NSCs, which may ensure recovery after long dry periods, as proposed by Martínez-Vilalta *et al.* (2016) in a global synthesis. This threshold supports a survival strategy of trees during dry conditions and it suggests NSC as an active sink (Silpi *et al*., 2007; Bustan *et al*., 2011; Sala *et al.* 2012). NSC dynamics also vary on a seasonal scale, responding to seasonal changes in soil water content (SWC) combined with temperature and vapor pressure deficit (VPD) and growth phenology, with maintenance of a minimum threshold of NSC content that may ensure recovery (Drossopoulos & Niavis, 1988; Bustan *et al*., 2011; Klein *et al*., 2014). Considering the higher frequency of drought events recorded in the last decades and their large effects on tree productivity and survival, NSC metabolism has a substantial role ensuring tree survival under stress (Bustan *et al*., 2011; Hartmann & Trumbore, 2016). Though its effect is potentially critical in understanding tree response to drought, carbon reserve allocation, regulation and effect on tree condition are not yet fully known (Mcdowell *et al.*, 2008; Allen *et al.*, 2010; Klein & Hoch, 2015; Lloret *et al.*, 2018).

Unlike *Arabidopsis* transient leaf starch metabolism, the molecular regulation of NSC storage as starch in woody tissues is poorly understood. While several steps within starch metabolism in leaves are probably conserved in sink tissues, some steps might be distinct to heterotrophic organs (Noronha *et al.*, 2018). The putative pathway in woody tissues begins with carbon transport to sink tissues as sucrose, deriving from source tissues. Sucrose is converted to glucose-6-phosphate through several stages and then transferred by glucose-6-phosphate/phosphate translocator to starch plastids (Kammerer *et al.*, 1998). In the plastid, it is converted into glucose-6-phosphate by phosphoglucomutase (PGM), then to ADP-glucose by ADP glucose pyrophosphorylase (AGP) and eventually into starch by starch synthase and starch branching enzyme (Fernie *et al.*, 2002; Noronha *et al.*, 2018). Starch can be modified by α glucan (Zhou *et al.*, 2017). When carbon shortage occurs, there are potentially multiple pathways by which starch may be degraded to soluble sugars, for example by α amylases, β amylases and other enzymes (Witt & Sauter, 1994; Smith, 2007; Zeeman *et al.*, 2010). Starch pathway studies in sink tissues have shown expression of enzymes involved in starch synthesis, as sucrose synthase (SUS), AGP and branching enzymes, and in starch degradation, such as starch phosphorylase, disproportionating enzymes (DPE), de-branching enzymes, α and β amylases, maltose translocators and glucose translocators (Smith *et al.*, 2005; Geisler-lee *et al.*, 2006; Regier *et al.*, 2009; Silva *et al.*, 2017; Noronha *et al.*, 2018). Additionally, the expression of starch degradation enzymes is higher in sink tissues following abiotic stress (Geisler-lee *et al.*, 2006; Regier *et al.*, 2009).

A combination between a molecular approach and physiological methods has been done mainly in *Arabidopsis thaliana* research (Sulpice *et al.*, 2009; Hummel *et al.*, 2010), however, it has been rarely done in tree's woody tissues, which constitutes the long-term storage tissues in long-lived plants. A few studies that have been concerned with a blend of starch-related gene expression with NSC content have been done focusing on several genes only, using reverse-transcription quantitative polymerase chain reaction (RT-qPCR) (Regier *et al.*, 2009; Pagliarani *et al.*, 2019). Despite the enduring interest in the molecular regulation of NSC metabolism in storage organs, knowledge is still limited about the genes involved in NSC synthesis and degradation following drought, and more so within large gene families. Our aim is to broaden current knowledge of starch metabolism in woody tissues and its relation to tree drought resistance mechanisms.

Olive (*Olea europaea* L.) is an evergreen broadleaf tree species, which is traditionally cultivated in rain-fed orchards in the Mediterranean basin (Loumou & Giourga, 2003). The prevalence of olives grown in arid and semi-arid areas, where plants are frequently subjected to high temperatures and droughts, indicates olives high resistance to water deficiency. This resistance also enables high metabolic activity in summer (as in fruit production). Even among other Mediterranean species, such as *Rosmarinus officinalis* L. and *Lavandula stoechas* L., olive responds better to soil drought across many indexes (Nogués & Baker, 2000). A series of strategies are suggested to assist in the drought resistance of olives, including a strong photosystem repair mechanism (Angelopoulos and Dichio, 1996), high regulation of stomatal conductance (Giorio *et al.*, 1999; Nogués & Baker, 2000; Rodriguez-Dominguez and Brodribb, 2019), osmotic adjustments (Dichio *et al.*, 2003, 2009; Bustan *et al.*, 2011) and a high water potential gradient between canopy and root system (Xiloyannis *et al.*, 1999). Furthermore, the drought resistance of olive is expressed by the ability to recover from a very low water potential (−6 MPa), showing the ability to adsorb up to a soil water metric of −2.5 MPa. This value is below the standard permanent wilting point of other trees, measured in a meta-analysis study at −2.3 MPa (Dichio *et al.*, 2003; Bartlett *et al.*, 2016). These strategies along with maintenance of a significant NSC threshold during drought in the olive suggest that starch degradation is also essential as a stress resistance strategy (Chapin *et al.*, 1990; Kobe, 1997; Bustan *et al.*, 2011). Elucidating the mechanisms allowing olives to bear prolonged droughts can facilitate our understanding of tree drought resistance in general. The olive tree is native to both orchards and forests in the Mediterranean, where it survives in naturally occurring dry conditions, and is hence a good model. Despite its relevance, the molecular regulation of NSC in olive in response to water shortage was not yet been investigated.

In this study, the water stress effect on NSC and starch regulation gene expression were tested in olive trees. During soil drying, photosynthesis gradually declines. During heat waves, VPD spikes and stomatal closure is enforced, regardless of soil conditions, and photosynthesis might shut down. In either separate or combined stresses, sink tissues such as branches and roots face contrasting needs both to store more carbon, while using existing reserves. During recovery from drought, carbon allocation to storage is often prioritized over growth (Wiley *et al.*, 2017), indicating storage importance in plant survival. Our research questions were: which genes involved in consumption of NSCs are differentially expressed (1) during an intensive abrupt heat wave? (2) during gradual soil drying? And (3) during recovery from soil drought? To address these questions, young olive trees grown outside in 25-l pots were exposed to limited water conditions and were monitored during drought and recovery. Confining study trees to pots allowed us to more fully regulate access to soil water than would have been possible with field-grown trees. The measurements included tissue concentrations of starch and soluble sugars, RNA expression levels of genes encoding enzymes involved in starch synthesis and degradation, leaf gas exchange and water potential. By analyzing these parameters simultaneously, we pointed to novel potential genes involved in this major metabolic pathway in olive trees, a drought-resistant species.

Materials and Methods

Plant material and climate

A group of 12 3-yr-old olive trees (*Olea europaea* L. cv Souri) was purchased from a local nursery and transplanted into 25-l pots in the Weizmann Institute in November 2017. The large pots were chosen to support root growth and overall plant development.

Planting soil was peat and tuff (50 : 50) and tree height was 1.6 m ± 0.1. Trees were kept outside under optimal irrigation of 1.2 l d^{-1} for a 5-month acclimation period. The experiment was conducted during May–July 2018. In April, before the experiment began, flowers were removed manually from trees to avoid fruit set and minimize variance between branches. Climate during the experiment was hot and dry with heat waves in May and a gradual increase in temperature during June (Fig. 1). Extreme temperatures (daily means of 30.5 to 32.7°C) were documented on days 8 and 12 of the water deficiency period, on the dates May 18 and 22, respectively. In these heat wave episodes, VPD increased to >3 kPa. During the whole period, mean temperature varied between 20.9 and 32.7°C (Fig. 1). Two rain events, of 4.8 mm each, took place during the experiment (in May). In the water deficiency period, the tree pots were covered to avoid water input from rain.

Experimental design

Six trees out of 12 were exposed to limited water conditions for 28 d. In the first 2 wk, dried trees were irrigated with 1 l wk^{-1} to enable gradual acclimation to the drought. From day 14 of the experiment, there was no irrigation for the dried trees for another 14 d. The timing of measurement days and re-irrigation was determined according to the tree's physiological conditions, considering their pre-drought levels of photosynthesis, stomatal conductance and water potential. The six watered trees were irrigated continuously with 1.2 l d^{-1}. Measurements were conducted on six campaign days: (1) 3 d before drought treatment (day −3, 7 May); (2)–(4) once a week following irrigation cessation (days 8, 13 and 27, on 07:00–09:00 h 18, 23 May and 6 June, respectively); (5) 3 d after re-irrigation (day 31, 10 June); and (6) at full recovery (day 80, 29 July), 52 days after re-irrigation. On each sampling day, material was collected and physiological measurements were performed at 07:00–09:00 h. Woody branches *c.* 15 cm long were collected after leaf and green shoot removal on all sampling days. Roots were collected on days −3, 27 and 80 only, in order to minimize disturbance to the soil and root system. Collected roots were *c.* 15 cm long. After collection, the tissues were ground, and aliquots from the same branches and roots were taken for the various assays (NSC and RNA measurements). The samples of branches and roots that were used constituted *c.* 0.1% of the tissue biomass, calculated by allometric equations based on tree height and diameter (Ruiz-Peinado *et al.*, 2012). Volumetric soil water content was measured on each measurement day with moisture sensors (EC-10; Decagon Devices, Washington, DC, USA).

Leaf gas exchange and water potential

During the experiment, leaf gas exchange, (i.e. transpiration and net assimilation) and water potential were measured once a week on 3–5 trees from each treatment to monitor the tree's physiological responses. Measurements were made with a Walz GFS-3000 photosynthesis system (Heinz Walz GmbH, Effeltrich, Germany), equipped with a lamp, set to a light intensity of 1000 μmol m^{-1} s^{-1} at ambient air temperature and humidity. Carbon dioxide (CO_2) was set to 400 ppm, matching ambient CO_2 levels. Gas exchange rates were further calibrated to the leaf actual area by scanning measured leaves and estimating projected leaf area. Gas exchange measurements were accompanied by leaf water potential (Ψ_l) using the pressure chamber technique (Scholander *et al.*, 1965). Woody branches of 5–7 cm long (after leaf and green shoot removal) were cut from three trees of each treatment (the trees that were used for gas exchange measurement) and put in a Scholander pressure chamber after the leaves were covered for 15 min (PMS Instrument, Albany, OR, USA) fed by a nitrogen gas cylinder. Gas pressure within the chamber was gradually increased (*c.* 1 MPa min^{-1}) until water emerged from the protruding cut branch surface, and the negative value of the pressure was recorded as the water potential (Ψ_l) in megapascals (MPa).

Nonstructural carbohydrate (NSC) analysis

The collected branch and root samples were powdered in liquid nitrogen with mortar and pestle, then lyophilized (Gamma 2-16 LSCplus; Christ, Osterode am Harz, Germany) for 48 h and ground again, using a Retsch Mixer Mill (MM301; Retsch GmbH, Haan, Germany), to a fine powder. Soluble sugar extraction was done by an adjusted protocol Quentin *et al.*, 2015. Sugars were separated in an analytical high-performance liquid chromatography (HPLC) system (Intelligent System; Jasco, Tokyo, Japan) fitted with a Sugar-Pak I column (6.5 mm × 300 mm; Waters, Milford, MA, USA) using a refractive-index detector (Kontron Instruments, Zurich, Switzerland). Starch was quantified according to Landhäusser *et al.*, 2018 by an enzymatic reaction involving hexokinase. An enzyme blend of glucose assay reagent (cat no. G3293-50ML; Sigma Aldrich, St Louis, MO, USA) was added to the final solution that was quantitatively analyzed using spectrophotometry by evaluating the accumulation of NADPH.

RNA extraction, library construction and RNA sequencing

Twenty-four branch samples were selected for transcriptome analysis: three trees each from each treatment group (watered trees: *Oe*3, *Oe*9 and *Oe*11, and dried trees: *Oe*4, *Oe*8 and *Oe*12) from four time points. The four time-points were day −3 (baseline), day 13 (heat wave and early drought), day 27 (late drought) and day 80 (post-drought). On days 13 and 27, the dried trees' assimilation was *c.* 15% and *c.* 0% out of pre-drought assimilation, respectively. RNA samples (branch and root) from the remaining trees and the sequenced trees were used for RT-qPCR measurements. Collected samples for RNA extraction were stored at −80°C and powdered with mortar and pestle in liquid nitrogen. Extraction was conducted according to Gambino *et al.* (2008), using cetyltrimethylammonium bromide (CTAB) (Gambino *et al.*, 2008). To adjust the extraction to the specific experiment and tissue (wood samples), a few modifications were made: samples were incubated at 65°C with CTAB for 25 min and saturated with lithium chloride (LiCl) overnight. RNA quantity was

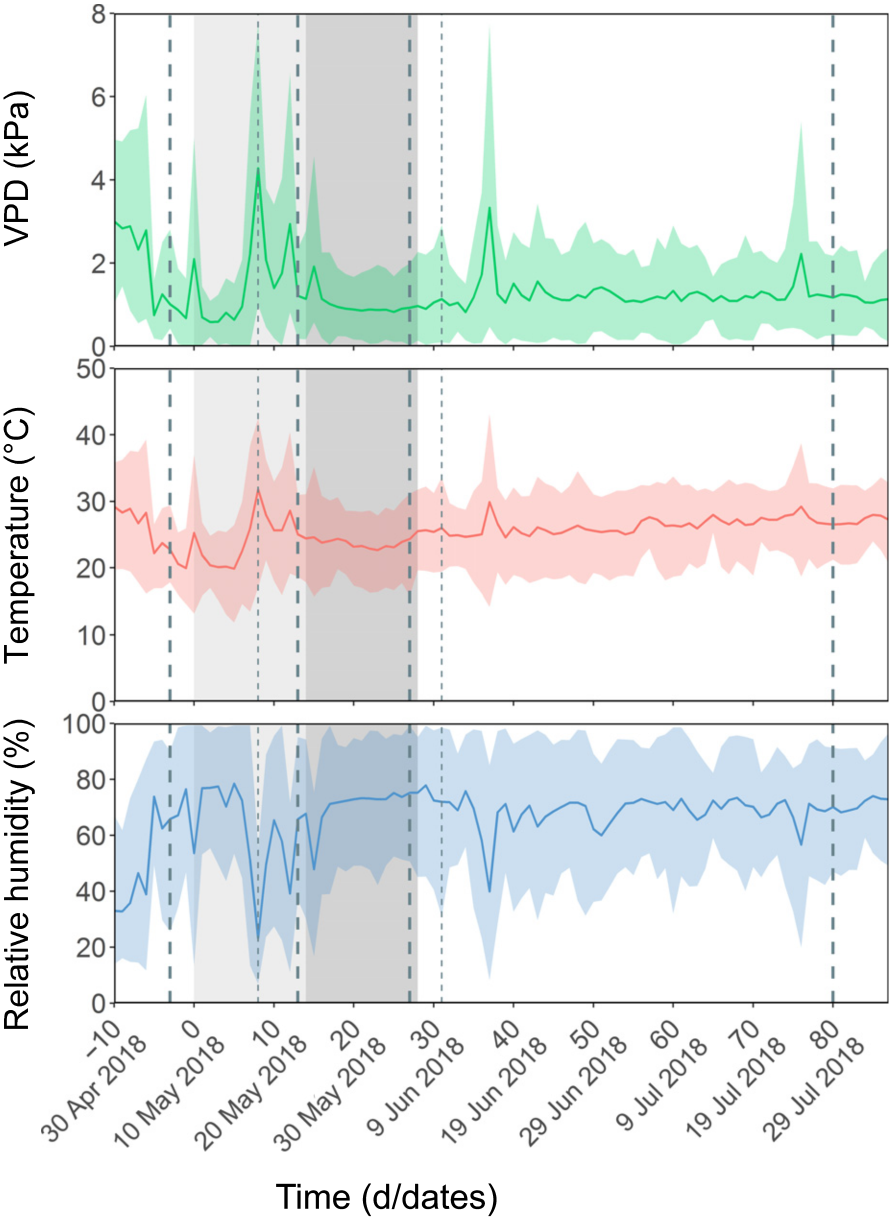

Fig. 1 Site meteorological conditions during the experiment: daily mean vapor pressure deficit (VPD; top); daily mean temperature (middle; including a seasonal trend line); daily mean relative humidity (bottom). Colored areas represent the range between daily maximum and minimum values. Gray shaded area represents water limitation period, with light gray (days 0–14) indicating drought acclimation and dark gray (days 14–28) indicating drought. Dashed vertical lines indicate time points of carbohydrate and gene expression measurements, with thick lines indicating RNA-seq measurements and thin lines indicating RT-qPCR measurements.

determined using a NanoDrop 1000 spectrophotometer (NanoDrop, Wilmington, DE, USA) and RNA quality was analyzed using the 2200 TapeStation System (Agilent Technologies, Santa Clara, CA, USA) according to the manufacturer's protocol. All RNA samples presented 260/280 and 260/230 purity and an RNA Integrity Number (RIN) > 5. Library preparation and sequencing was done by the Genomics Unit at the Grand Israel National Center for Personalized Medicine (G-INCPM) at the Weizmann Institute of Science (Rehovot, Israel). Libraries were constructed with barcodes to allow multiplexing of all 24 samples in one lane, including three branch samples from each treatment (watered and dried) from four time points. Two lanes with all samples were sequenced. Between 10 and 20 million single-end 60-bp reads were sequenced per sample using an Illumina HiSeq 2500 V4 instrument.

Manual sequence curation, transcriptome assembly, and enrichment analysis

A full description of the applied bioinformatic methods is included in the Supporting Information (Methods S1). Briefly, 19 enzyme families involved in sucrose metabolism, starch metabolism and starch degradation were selected (Fernie *et al*., 2002; Smith, 2007; Noronha *et al*., 2018). Known sequences of the selected enzymes were found in the Kyoto Encyclopedia of Genes and Genomes (KEGG) pathway database. All protein sequences were compared to genomes from olive and other tree species, and to an unpublished genome of *Olea europaea* L. cv Souri, created by Dr Ben-Ari (ARO). The final DNA sequences are included in Table S1, and the number of members in each family are presented in Table 1. A new gene set was built integrating the manually curated genes with the automated annotation. Differentially expressed (DE) genes from baseline values (unless specified differently), were identified by applying the DESeq2 program (Love *et al.*, 2014). The final DESeq2 analysis is available as Table S2. Gene ontology (GO; Table S3) and KEGG orthology (KO) annotations were obtained from the Joint Genome Institute (JGI) portal. Finally, a phylogenetic tree was constructed with related genes from a wide variety of plant species (Methods S1). Details of the sequences used in this phylogenetic tree are included in Table S4.

cDNA synthesis and gene expression analysis by qPCR

From each time point 8–12 RNA samples, including not sequenced samples, were treated with RQ1 RNase-free DNase (Promega, Madison, WI, USA) according to the manufacturer's instructions. Complementary DNA (cDNA) was synthesized with the qScript cDNA synthesis kit (Quanta Biosciences, Gaithersberg, MD, USA). Reactions were conducted using Fast SYBR® Green master mix (Applied Biosystems, Foster City, CA, USA) on QuantStudio 5 Real-Time PCR System, 384-well (Applied Biosystems) in triplicates. To determine ΔCT, samples were normalized to the housekeeping gene ATPase (ATPase, V0/A0 complex, subunit C/D), the most stable gene in RNAseq results. ΔΔCT was determined by subtracting ΔCT of day −3 out of ΔCT of the current measurement day for each tree.

Statistical analysis

Data of leaf gas exchange, water potential, NSC and RT-qPCR were statistically analyzed using the nonparametric Mann–Whitney test with Bonferroni correction, to determine significant differences between dried and watered trees in each measuring day. NSC measurements were also analyzed by Kruskal–Wallis test with Bonferroni adjustment, comparing samples from different days of the same tissue and treatment. These tests were conducted with the software R (v.3.1; the R Foundation for Statistical Computing, Vienna, Austria), using the packages AGRICOLAE (v.1.3-0, 2019) for the Kruskal–Wallis test and R STATS core package for the Mann–Whitney test. Principle component analysis (PCA) was performed with R STATS core package, including missing data correction by the package MISSMDA (v.1.13, 2020) based on Dray & Josse (2015). Statistical tests for the gene expression levels are detailed in the respective sections earlier.

Results

Physiological response to water limitation

Dried trees showed a sharp decrease in leaf gas exchange along with a decline in leaf water potential, in correspondence with SWC decrease. Watered trees SWC fluctuated slightly throughout the experiment due to heatwaves, yet still differed from dried trees, where SWC decreased sharply during drought (Fig. 2a). Water potential of dried trees became more negative in drought, in correspondence to SWC, two-fold and six-fold less than watered trees in days 13 and 27, respectively. Three days after re-irrigation, water potential increased from −8.23 MPa at day 27 to −1.19 MPa (Fig. 2b). Among leaf gas exchange results, assimilation of watered trees showed a rather stable trend, increasing from 14.7 μmol m^{-2} s^{-1} at day 8 to 24.3 μmol m^{-2} s^{-1} at day 20. In dried trees, assimilation decreased from 13.4 μmol m^{-2} s^{-1} on day −3 to 0.5 μmol m^{-2} s^{-1} on day 27 (the last day of water limitation) (Fig. 2c). These differences mean that the assimilation rate in dried trees was 29%, 8% and 2% of the assimilation of watered trees on days 7, 20 and 27, respectively. Three days after re-irrigation, the assimilation rate of dried trees matched that of watered trees. The changes in

Table 1 Number of genes within each of the 19 manually curated gene families.

Process	Gene name	Number	Catabolism/anabolism
Sucrose metabolism	Invertase	11	Catabolism
	Hexokinase	9	Anabolism
	Sucrose synthase	12	Catabolism
	UDP-glucose pyrophosphorylase	2	Anabolism
	Phosphoglucomutase	4	Anabolism
	Glucose-phosphate translocator	5	Catabolism and anabolism
Starch synthesis	ADP-glucose pyrophosphorylase	8	Anabolism
	Starch synthase	9	Anabolism
	Starch branching enzyme	5	Anabolism
Starch degradation	Isoamylase	3	Catabolism
	α-Glucan	2	Anabolism
	α-Amylase	5	Catabolism
	β-Amylase	13	Catabolism
	Disproprtionating enzyme	2	Catabolism
	Starch phophorylase	4	Catabolism
	Maltose transporter	3	Catabolism and anabolism
	Glucose transporter	1	Catabolism and anabolism
Polyol metabolism	Polyol transporter	3	Catabolism and anabolism
	Mannose-6-phosphate reductase	2	Anabolism

transpiration rate demonstrated the same patterns, albeit with increased transpiration in the last part of the experiment, and more so in re-irrigated trees (Fig. 2d).

NSCs in branches and roots

The largest drought responses amongst stored NSCs were the increase in mannitol and decrease in starch in branches of the dried trees. Total NSCs in branches was similar across dried and watered trees, in that it had a decrease on day 8 and an increase in summer. However, NSC component partitioning differed between watered and dried trees (Fig. 3). The watered trees soluble sugar concentration was steady, while starch fluctuations contributed the most to the seasonal changes. In dried trees, starch percent dropped to 0% dry matter (DM) at days 8 and 27, with a minor increase in day 13 to 0.3% DM. On day 8, there was no significant difference between watered and dried trees. Mannitol was the main NSC component through all treatment days, up to 71% of total NSCs on day 27. Likewise, sucrose showed the same pattern as mannitol with a lower peak. By contrast, glucose and fructose in dried trees resembled watered trees in all time points except day 31 (3 d after re-irrigation), when they increased, though not significantly, by a factor of two and seven, respectively, compared to watered trees on the same day. NSC patterns in roots showed a smaller effect of the drought and re-irrigation than in branches. Starch in the dried tree roots showed a decreasing trend through the drought period, although not significantly different from watered trees on the same day. To summarize the overall effects of all of the various factors (physiological conditions, weather, etc.) PCA was performed on all of the conditions together, and revealed that physiological and weather conditions had a strong influence of VPD on NSCs and leaf gas exchange on day 8, while other measurement days were mostly influenced by SWC (Fig. S1).

Transcriptional changes in branches following water limitation

To study the dynamics of the molecular changes under drought stress and during recovery, DE genes were grouped into three clusters based on their expression trend along the course of the experiment (Fig. 4a). Cluster 1, with 5477 genes, displayed genes with persistent downregulation during drought and upregulated in recovery; cluster 2 (1397 genes) displayed genes downregulated increasingly throughout drought days and upregulated in recovery; and cluster 3 (5250 genes) displayed genes with higher expression during drought. GO enrichment analysis was performed on DE genes in all three clusters (Fig. 4b; for full data see Table S3). Among the enriched biological functions with a highly significant P-value ($P < 0.01$), which were assigned to clusters 1 and 2, we identified numerous processes related to starch metabolism. These included starch catabolic process,

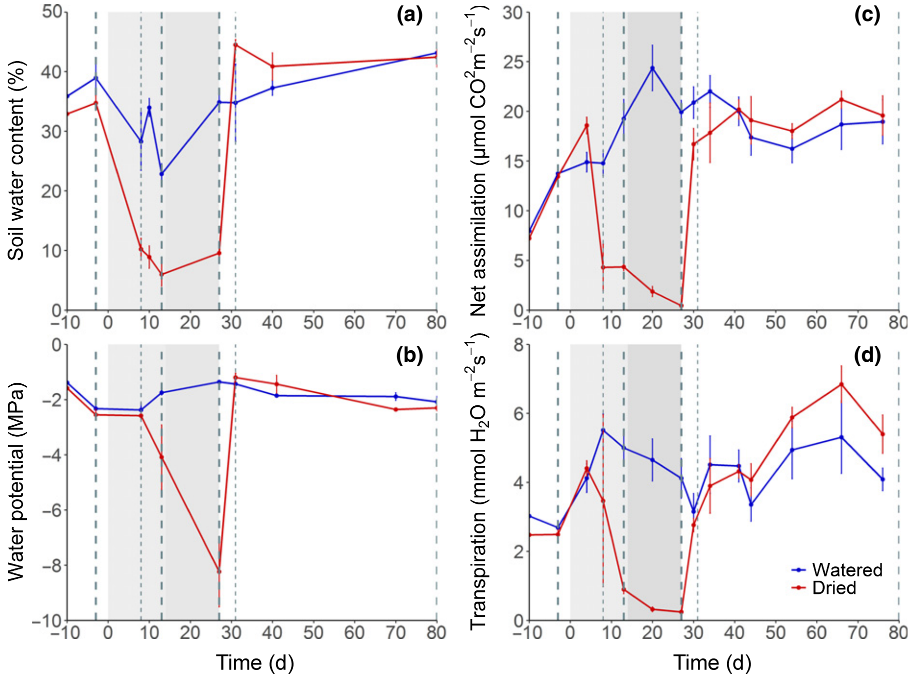

Fig. 2 Changes in soil water content ($n = 6$ except for day 38, $n = 2$) (a), water potential ($n = 3$–4) (b), rate of assimilation ($n = 3$–5) (c), and rate of transpiration ($n = 3$–5) (d) of dried and watered *Olea europaea* trees. Each value represents a mean of number of trees, represented by a number next to the point. Between one and two leaves were collected from each tree. The *x*-axis represents the number of days from the beginning of treatment. Gray shaded area represents water limitation period, light gray (days 0–14) indicates drought acclimation and dark gray (days 14–28) indicates drought. Dashed vertical lines indicate time points of carbohydrate and gene expression measurements, where thick lines in gene expression measurements indicate RNA-seq measurements and thin lines indicate RT-qPCR measurements. Error bars indicate SE.

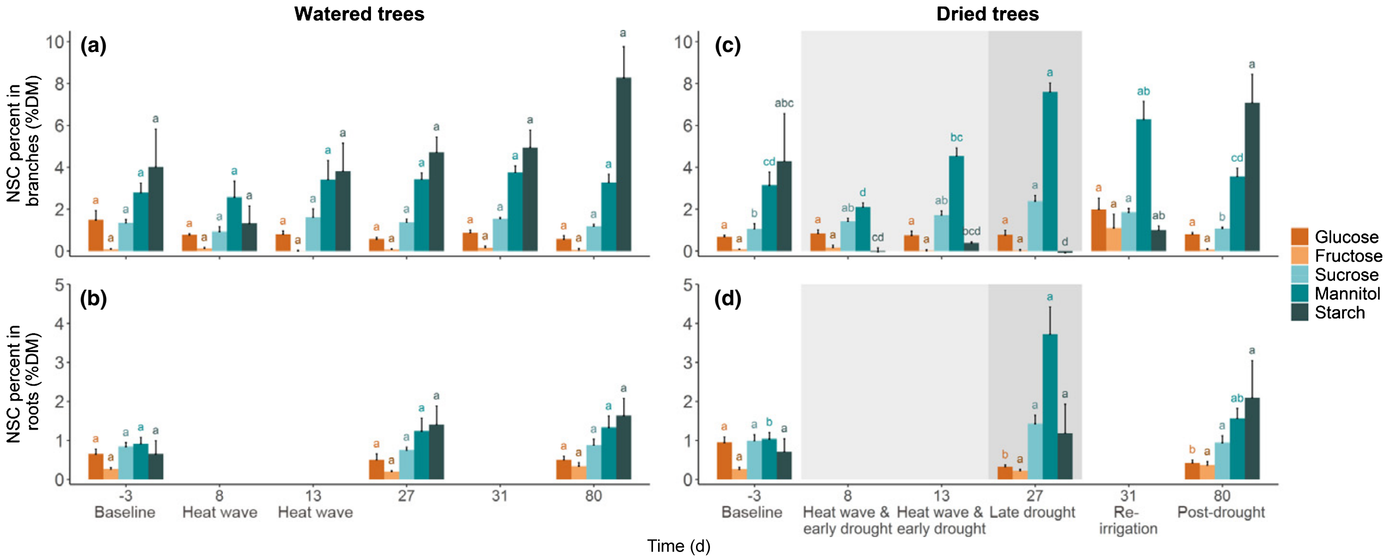

Fig. 3 The effect of water limitation period on nonstructural carbohydrate (NSC) content (in percent of dry matter; DM) in branches ((a), (c); $n = 4–6$) and roots ((b), (d); $n = 5–6$) of *Olea europaea*. Bars indicate NSC content (glucose, fructose, sucrose, mannitol and starch). Gray shaded areas represent water limitation period, where light gray indicates drought acclimation and dark gray indicates drought. Results of Kruskal–Wallis test, which compared between the days of each treatment and tissue, are shown above each bar. Different lowercase letters are significantly different ($P < 0.05$). Error bars represent SE.

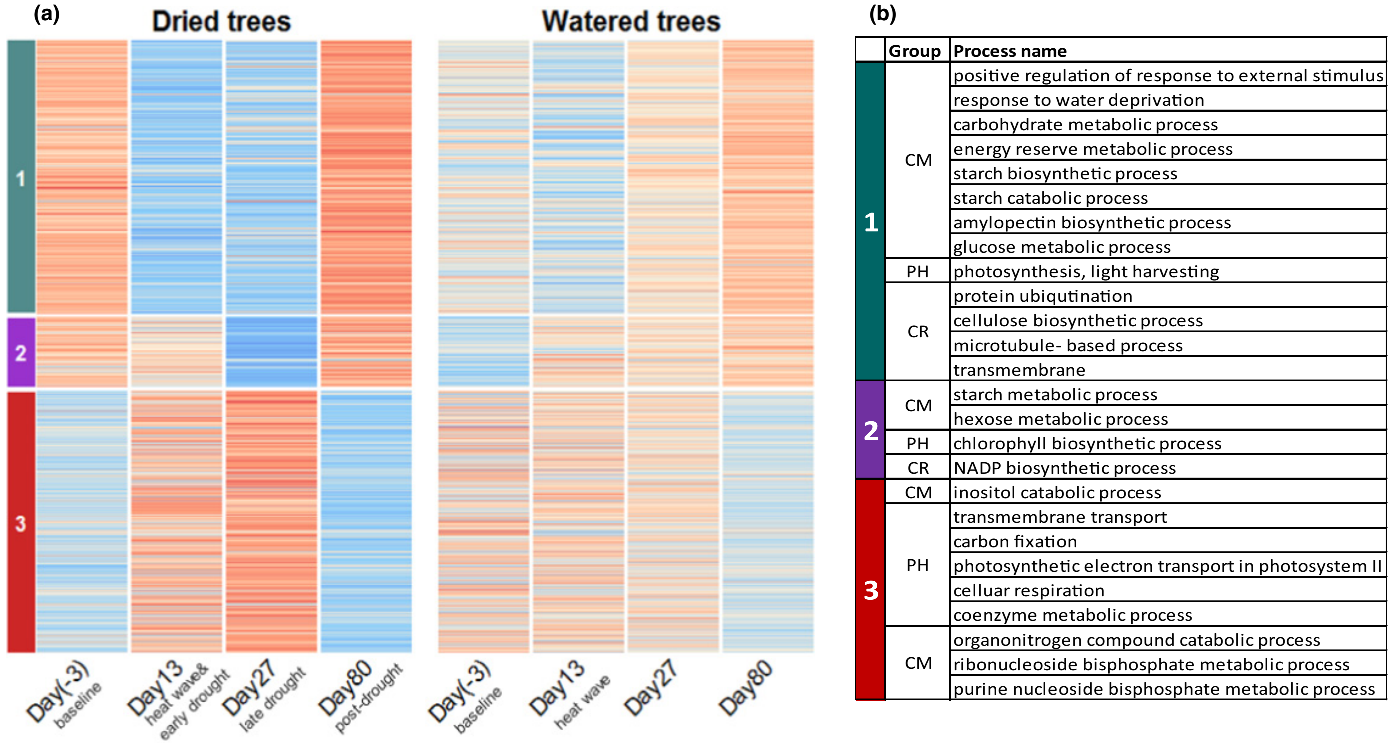

	Group	Process name
1	CM	positive regulation of response to external stimulus
		response to water deprivation
		carbohydrate metabolic process
		energy reserve metabolic process
		starch biosynthetic process
		starch catabolic process
		amylopectin biosynthetic process
		glucose metabolic process
	PH	photosynthesis, light harvesting
	CR	protein ubiquitination
		cellulose biosynthetic process
		microtubule- based process
		transmembrane
2	CM	starch metabolic process
		hexose metabolic process
	PH	chlorophyll biosynthetic process
	CR	NADP biosynthetic process
3	CM	inositol catabolic process
	PH	transmembrane transport
		carbon fixation
		photosynthetic electron transport in photosystem II
		celluar respiration
		coenzyme metabolic process
	CM	organonitrogen compound catabolic process
		ribonucleoside bisphosphate metabolic process
		purine nucleoside bisphosphate metabolic process

Fig. 4 (a) Heatmap based on clustering of 12 124 differentially expressed genes in dried and watered *Olea europaea* branches. Orange and blue bars represent positive and negative changes, respectively, and the intensity of the color represents the normalized $\log_2$ expression level at each stage (days −3, 13, 27 and 80) for the mean of three sequenced trees in each treatment. Each gene was normalized to itself. (b) Significantly enriched biological functions ($P < 0.01$; partial list) related to clusters as displayed in (a). Colors indicate clusters as in (a). For a full list of enriched biological pathways in each cluster, see Supporting Information. Functions were divided into groups as following: carbohydrates metabolism (CM), photosynthesis (PH) and cellular regulation (CR).

amylopectin biosynthesis and glucose metabolic process. Cluster 3 contained, among others, processes involved in inositol metabolism and in cellular respiration.

Differentially expressed genes under soil drought

Volcano plots of DE genes in dried trees compared to watered trees were drawn according to the DESeq2 results, where DE genes had a false discovery rate (FDR) lower than 0.05 (Fig. 5; for full data see Table S2). On day 13 (heat wave and early drought) following water cessation, 72 DE genes were upregulated and 42 were downregulated, e.g. genes related to cell wall synthesis (polygalacturonase) and protein degradation (aspartyl protease), in dried trees compared to watered trees. On day 27 (late drought), by contrast, 1348 DE genes were upregulated and 1195 DE genes were downregulated (dried vs watered trees). Among the upregulated genes were genes related to cell wall synthesis (polygalacturonase inhibitor 1-related and chitinase), alcohol degradation (alcohol dehydrogenase), sugar transport (sucrose transporter SWEET15), ethylene biosynthesis (methionine adenosyltransferase and aminocyclopropanecarboxylate oxidase), ABA synthesis (β glucosidase) and stress related proteins (dehydrins). On day 80 (post-drought), only seven genes were DE, 5 and 2 upregulated and downregulated, respectively. Four of the genes had unknown function, while genes such as amino acids transporters and cytochrome P450 were upregulated. In summary, the largest number of DE genes were found on day 27, while on days 13 and 80 the number of DE genes was 22-fold and 363-fold less than on day 27, respectively.

Expression patterns of starch regulation genes

RNA-seq results regarding starch regulation genes generated some interesting results in terms of DE genes and their expression trends along the drought period. Eighty-nine genes were expressed in branch tissue out of 103 manually curated genes (shown in Table 1). Among these, 59 were DE within at least one comparison out of the DESeq2 comparisons between all measurement days and treatments (Fig. 6). We identified the carbon storage process gene family members relevant to drought stress conditions. Among genes related to the starch synthesis process, four genes were significantly upregulated in dried trees on day 13 (heat wave and early drought) as compared to day −3 (baseline): starch synthases 2, 3, 4 and α glucan 2 (FDR < 0.05). Starch branching enzyme (SBE) was also upregulated in dried trees in day 13 (early drought), compared to day 27 (late drought). In addition, starch synthase 3 expression was significantly induced on day 13 (heat wave and early drought) in watered trees, along with a significant downregulation of AGP 2 (Fig. 6) (day 13, heat wave, compared to day −3, baseline, in watered trees, FDR < 0.05). Other starch synthases, such as starch synthase 1 and 8, were significantly downregulated throughout water limitation and were upregulated only at the end of recovery. Additional drought-induced downregulated starch synthesis genes were AGP 1, 2, 5 and 6.

The starch degradation drought-induced genes were upregulated throughout the drought period, (days 13 and 27 compared to baseline values), with downregulation in recovery. This group includes β amylases 2 and 10 (Fig. 7), along with Polyol transporter 2. By contrast, other family members of β amylase, such as β amylase 12, were downregulated in drought, followed by upregulation in recovery. In order to compare the olive β amylase genes to others with known functions from other plant species, a phylogenetic tree was constructed (Fig. S2). *O. europaea*'s β amylases 2 and 10 are homologs of *A. thaliana* β amylase 9, in clade V (Thalmann *et al*., 2019). Another essential phase in starch metabolism includes sucrose-related genes that are involved with sucrose metabolism before glucose-6-phosphate enters the amyloplast. Sucrose-related genes are expressed in different patterns. The first was drying-induced upregulation, which persisted throughout the drought period in invertase 11, along with a significant upregulation in day 27 (compared to well-watered trees)

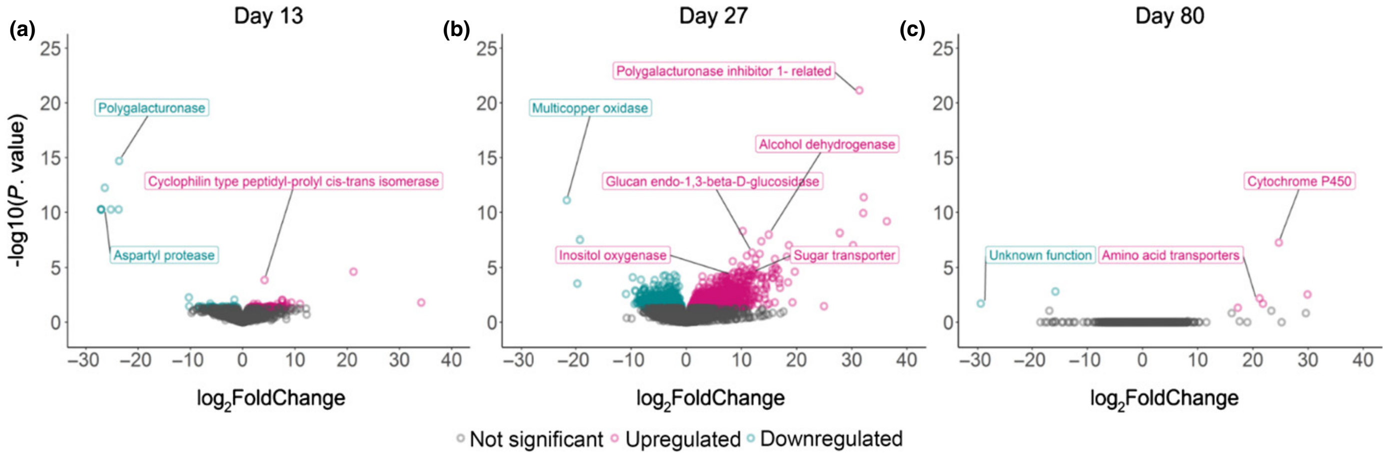

Fig. 5 Summary of changes in gene expression in response to drought as measured by RNA-seq analysis of *Olea europaea* branches. Volcano plots with gene expression ratios ($\log_2$ fold change) plotted against the negative $\log_{10}$-transformed *P*-values from a *t*-test calculation. Fold changes were calculated by the DESeq2 program. Gene expression ratios are shown between dried and watered trees on day 13 (a, heat wave and early drought), day 27 (b, late drought) and day 80 (c, post-drought). Significantly upregulated genes with false discovery rate (FDR) < 0.05 are shown as pink spots, downregulated genes are shown as blue spots and nonsignificant genes are shown as gray spots.

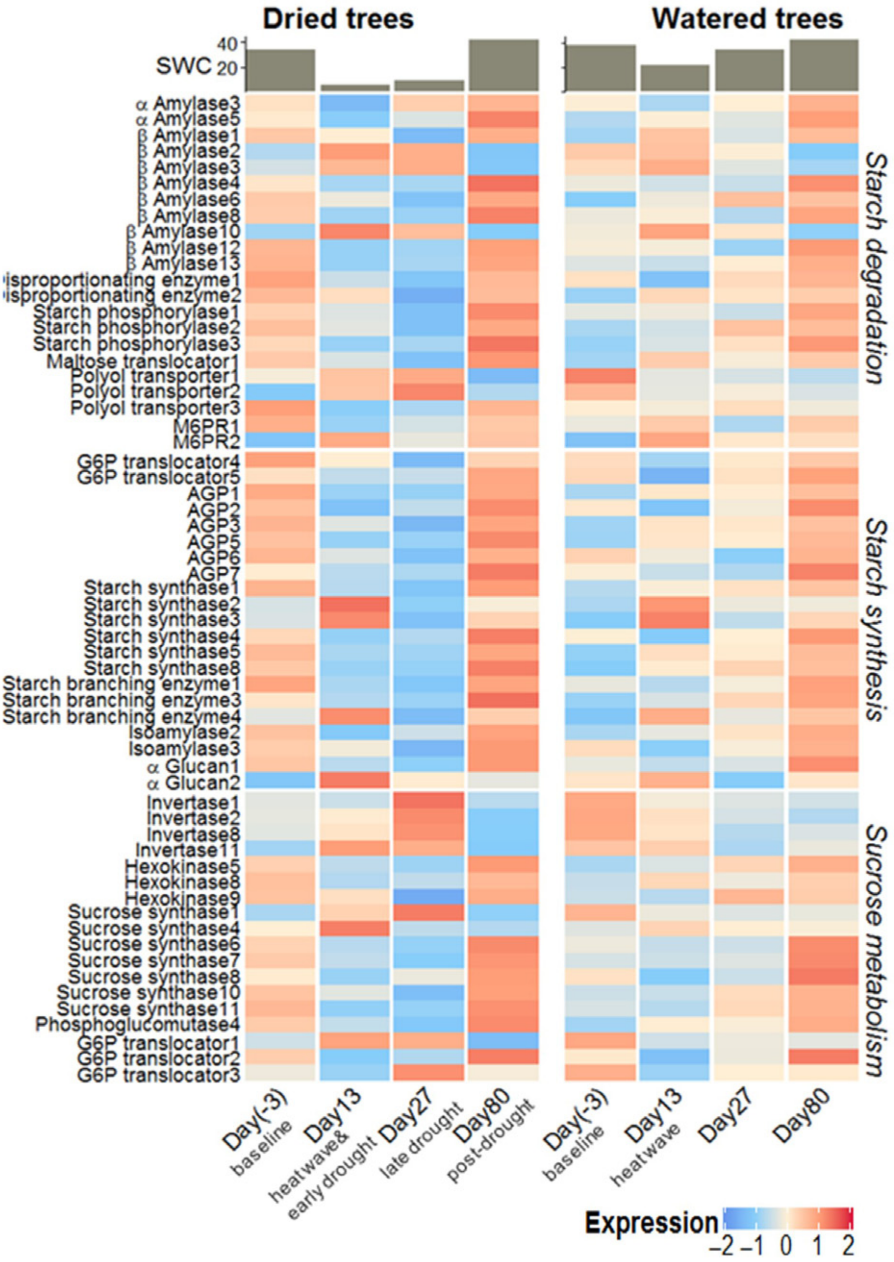

Fig. 6 Heatmap diagram showing the seasonal and drought-related dynamics of differentially expressed starch regulation genes in branches of watered and dried trees. Differentially expressed genes in at least one DESeq2 comparison were included. Red and blue represent positive and negative changes, respectively. Intensity of the color represents the normalized $\log_2$ expression level at each stage (days −3, pre-drought; day 13, heat wave; day 27, late drought; day 80, post-drought) for the mean of three sequenced samples in each treatment. Bars on top represent soil water content (SWC) on each day for the mean of three sequenced trees in each treatment.

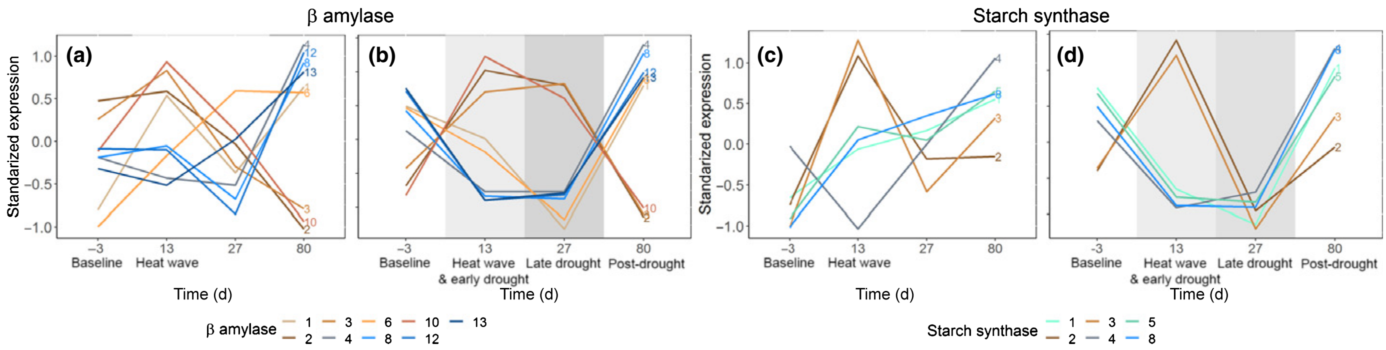

Fig. 7 Profile of normalized expression of β amylases of watered (a) and dried trees (b), and starch synthases of watered (c) and dried trees (d) in *Olea europaea* branches. Each line represents mean normalized $\log_2$ expression level of three trees across experiment days. Gray shaded areas represents the drought period, where light gray indicates drought acclimation and dark gray drought. Colors indicate different members in the gene family.

in invertases 1, 2, 8 and SUS 1. Another pattern exhibited was downregulation of SUSs 6, 7, 10 and 11 as compared to baseline values.

Recovery of dried trees was clearly demonstrated at the molecular level, with 49 differentially expressed genes, 38 of them upregulated. In watered trees, no significant changes in gene expression were observed between day 80 and day 27. Among recovered trees, genes that were significantly upregulated were related to starch synthesis (starch synthases 1, 4, 5, 8 and AGPs 1, 2 and 5) as well as starch degradation genes (starch phosphorylases 1, 2 and β amylases 1, 4, 6, 8 and 12). To summarize the expression patterns of starch regulation genes, partitioning among gene families was observed, where some members of the families of starch synthase, β amylase and polyol transporter were upregulated following drought (while other members were showed the opposite). Upregulation during drought was followed by downregulation in recovery (which families?).

Quantitative PCR (qPCR) was used to validate treatment-specific expression patterns in six differentially expressed genes with the addition of root gene expression measurements (Fig. 8). All tested genes exhibited expression patterns that were consistent across the two platforms. However, there were slight differences: β amylase 10 expression in watered trees was higher in RT-qPCR than RNA-seq. In addition, polyol transporter 1 expression increased on day 27 in qPCR, and not on day 13, as seen in RNA-seq.

Correlations between expression of starch metabolism genes and their substrates

To integrate metabolites and gene expression in response to drought, correlation between expression of starch metabolism genes and their putative substrates or products were examined. A positive correlation was demonstrated between the starch synthase family genes to starch amount. The highest R^2 was assigned to starch synthase 4 (0.499; $P = 0.0005$), followed by starch synthases 8 and 1. Starch synthases 2 and 3 had low coefficients, though also positive, compared to the other genes in their family (Fig. 9a,d). Five out of 13 β amylases had negative correlations with starch amount, similar to their coefficients (Fig. 9b,d). Further, there was a correlation with three polyol transporters, putative transporters of mannitol, the highest sugar in olive drought response. All three of them showed positive correlation with mannitol amount. The highest R^2 among these correlations was 0.478, for polyol transporter 2, indicating that it probably has the main role in mannitol transport to the olive branches. (Fig. 9c,d). In conclusion, correlation between gene expression and their substrate or product was shown in three genes, including starch synthase 4, β amylase 2 and polyol transporter 2, suggesting their role in olive's starch metabolism under drought.

Discussion

In this research, we present a novel combination of physiological, biochemical and molecular approaches to study carbon management under water deficiency in trees, and specifically in *O. europaea*. The relationships between molecular and biochemical responses, supported by physiological responses, sharpen our knowledge about the role of starch metabolism in olive's survival strategies under drought. We show that the day-to-day gene expression of the starch metabolism machinery is distinct from stress-mode, with specific genes being uniquely expressed due to the stress-mode response in olive storage tissue. The identification of stress-specific genes within the manually built gene families indicate that these genes are good candidates for further study, which can contribute to the effort of finding or even designing drought protected forest trees, or, alternatively, faster growing fruit trees (by decreasing the activity of starch synthesis genes in favor of growth). Pinpointing the specific enzymes responsible for carbon reserve management under heat, drought, and recovery, is also critical to deciphering tree mortality mechanisms (McDowell *et al.*, 2008; Mitchell *et al.*, 2013). A discussion of transcriptomic changes in other carbon metabolism genes, other than starch, in olive under drought is included in the Notes S1.

Identification of the gene family members related to starch synthesis and degradation processes under stress based on their expression

Our results distinguish gene family expression patterns between irrigated and drought conditions. On day 13 (heat wave and early drought), an upregulation in dried trees was observed among several starch synthesis genes as starch synthases 2, 3, 4, α glucan 2 and SBE 4. Starch synthase 3 expression was also significantly induced by heat alone, i.e. in watered trees. In examination of the starch metabolism from a whole process perspective, based on available literature (Fernie *et al.*, 2002; Smith *et al.*, 2005; Noronha *et al.*, 2015), the genes mentioned earlier are assigned to families involved in the final stages of starch synthesis and modifications (starch synthases, α-glucans and SBEs; Fig. 10). This upregulation, followed by downregulation on day 27, might be the response to a heat wave of three different gene families involved in the same process of starch synthesis. As for the starch synthase family specifically, so far it was shown to be differentially expressed following cold stress in *O. europaea* leaves (Guerra *et al.*, 2015; without information on specific genes) and after leaf removal in grapevine canes (Silva *et al.*, 2017). Our results provide an answer to the first research question, regarding gene expression following heat wave, demonstrating divergent expression trends and further differentiating between the response to soil drought and heat in a long-term storage tissue. Upregulated starch synthases on day 13 (heat wave) of watered trees had the same pattern as dried trees but with a lower peak. This gap between the treatments reflects the regulation difference between early drought and VPD effects, when both effects induced higher expression of several starch synthases.

The question of low starch content simultaneously with upregulation of some starch synthesis genes needs further investigation. One explanation might be the mild increase in starch amount, from 0% on day 8 to 0.3% on day 13 (Fig. 3). High expression of starch synthases accompanied by high expression levels of

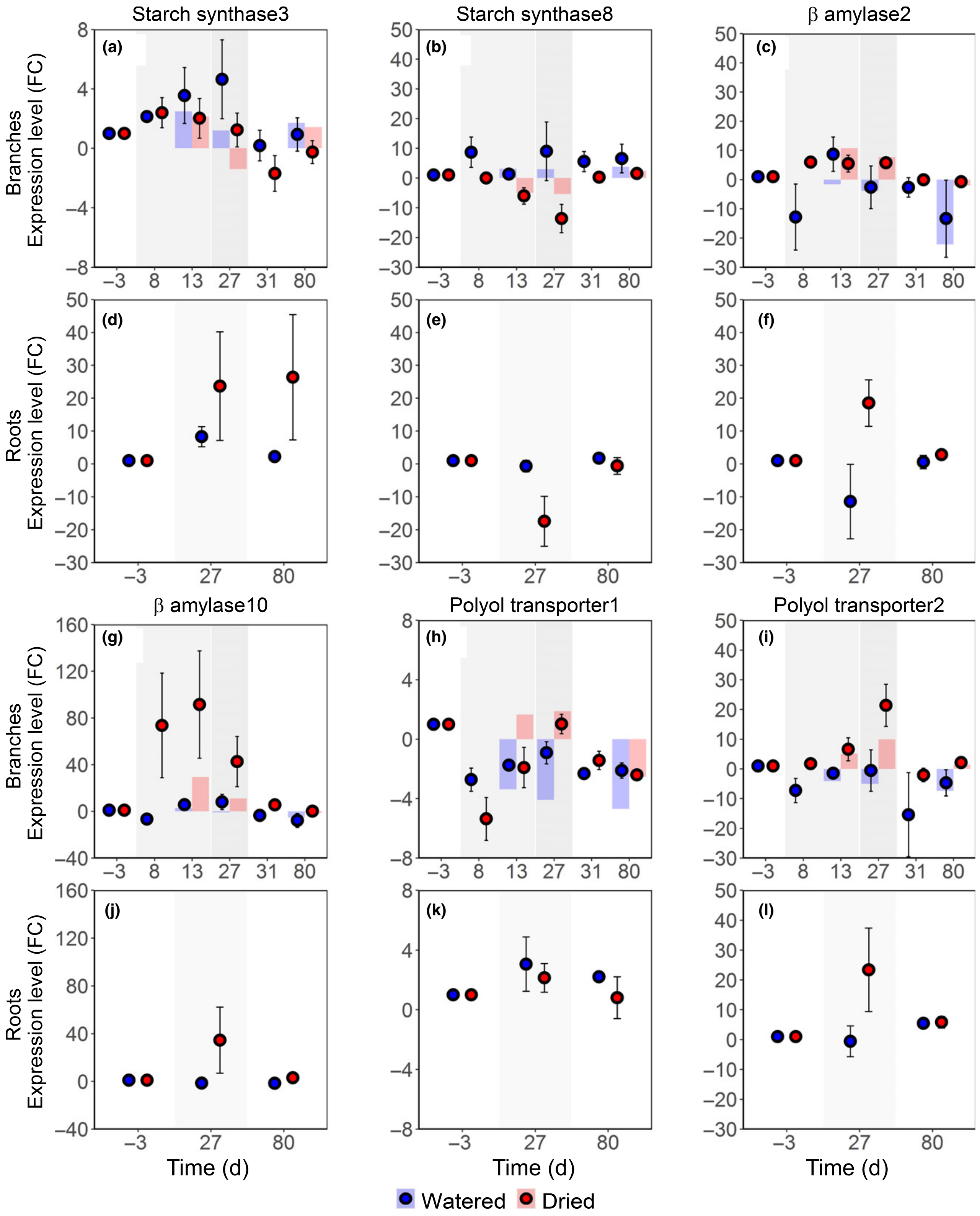

Fig. 8 Gene expression of selected genes along six and three measuring days in (a–c, g–i) branches and (d–f, j–l) roots, respectively. Bars indicate expression measured in RNA-seq and points indicate expression measured in RT-qPCR. All RT-qPCR values are the mean of three to six samples, relative to day −3. Gray shaded areas represents the drought period; light gray indicates drought acclimation and dark gray drought. In (d -f, j -l), the gray area represents drought only. Blue and red represent watered and dried trees, respectively. Error bars indicates SE of RT-qPCR.

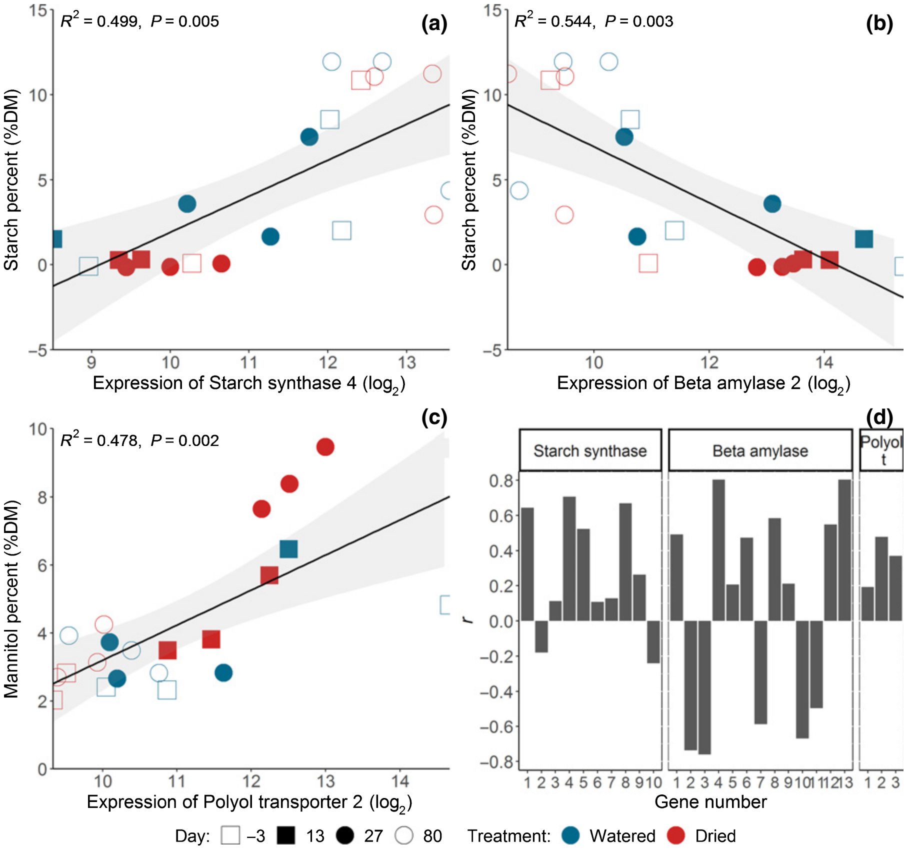

Fig. 9 Correlations between enzyme gene expression level and substrate concentration in wood of *Olea europaea*. Data points are for individual trees on specific days; shapes indicate the day. The *P* values are corrected with 'Bonferroni' depending on gene family's size. (a) Starch content as a function of starch synthase 4 expression. (b) Starch content as function of β amylase 3 expression. (c) Mannitol content as function of Polyol transporter 2 expression. (d) Levels of coefficients of correlation (*r*) of gene expression levels with the enzyme substrate or product in the three gene families.

starch degradation enzymes is a possible reason for the mild increase. The increase in a futile cycle is also suggested, supported by expression of both anabolic and catabolic genes. Furthermore, NSC location within the wood reflects NSC age, where younger NSC is mixed inwards while older NSC is used (Trumbore *et al.*, 2015; Hartmann & Trumbore, 2016; Furze *et al.*, 2018). Hence, simultaneous expression of the opposite processes might appear within different wood areas, where starch degradation takes place in the center of the stem and starch synthesis occurs in the peripheral area. In addition, the branch is composed of multiple cell types, including xylem, parenchyma, phloem, etc., which were not separated in this experiment. Differentiating between specific tissues and cells type might affect gene expression along with NSC content, and hence should be considered in future research. Another alternative is that unmeasured post-transcriptional processes were involved in these mechanisms, as differences between the RNA and enzyme level or activity do exist, as was shown in yeast (Gygi *et al.*, 1999). However, the high correlation presented here between the expression of specific genes and their substrate or product supports their role in affecting the substrate or product abundance.

In response to our second research question, change in genes expression in response to drought, persistent responses to drought took place among different starch metabolism processes. Drought-induced upregulation included starch degradation genes in wood, being the major tree carbon reserve. Upregulation of β amylases 2 and 10 during drought matched the observed starch decrease (Fig. 9); these genes homolog (β amylase 9) is predicted to be catalytically inactive, and had no defined functions in other studies, although it is close to a branch of another inactive enzyme, β amylase 4, which is proposed to have a regulatory role (Fulton *et al.*, 2008; Thalmann *et al.*, 2019). *Arabidopsis thaliana* lacking β amylases 3 and 9 was shown to accumulate more starch than plants lacking β amylase 3 alone, suggesting β amylase 9 has a role in starch metabolism in *Arabidopsis* (Monroe & Storm, 2018). A mild upregulation of PtBMY3, which belongs to class V (BAM9) as well, was shown in poplar branches (Pagliarani *et al.*, 2019). Another increase of β amylase isoforms in *O. europaea*'s leaves was shown following cold stress (Guerra *et al.*, 2015). Though β amylase 1 in poplar storage tissues was highly differentially expressed (Geisler-lee *et al.*, 2006; Pagliarani *et al.*, 2019), its homolog in our experiment has shown no changes during drought (β amylase 11). This difference might be due to the variance between the species. In our study, all upregulated β amylases were significantly downregulated in recovery, while other family members followed the opposite trend of upregulation through recovery. Furthermore, changes in gene expression of *O. europaea* β-amylases highly correlated to its substrate quantity, as was demonstrated previously in *A. thaliana* leaves (Kaplan & Guy, 2004). Other starch degradation genes were mostly downregulated, as shown in Fig. 10 (e.g. isoamylase 3, DPE 3 and maltose translocator 1). The exceptional upregulation of some β amylases among all starch degradation genes indicates their major contribution during drought response.

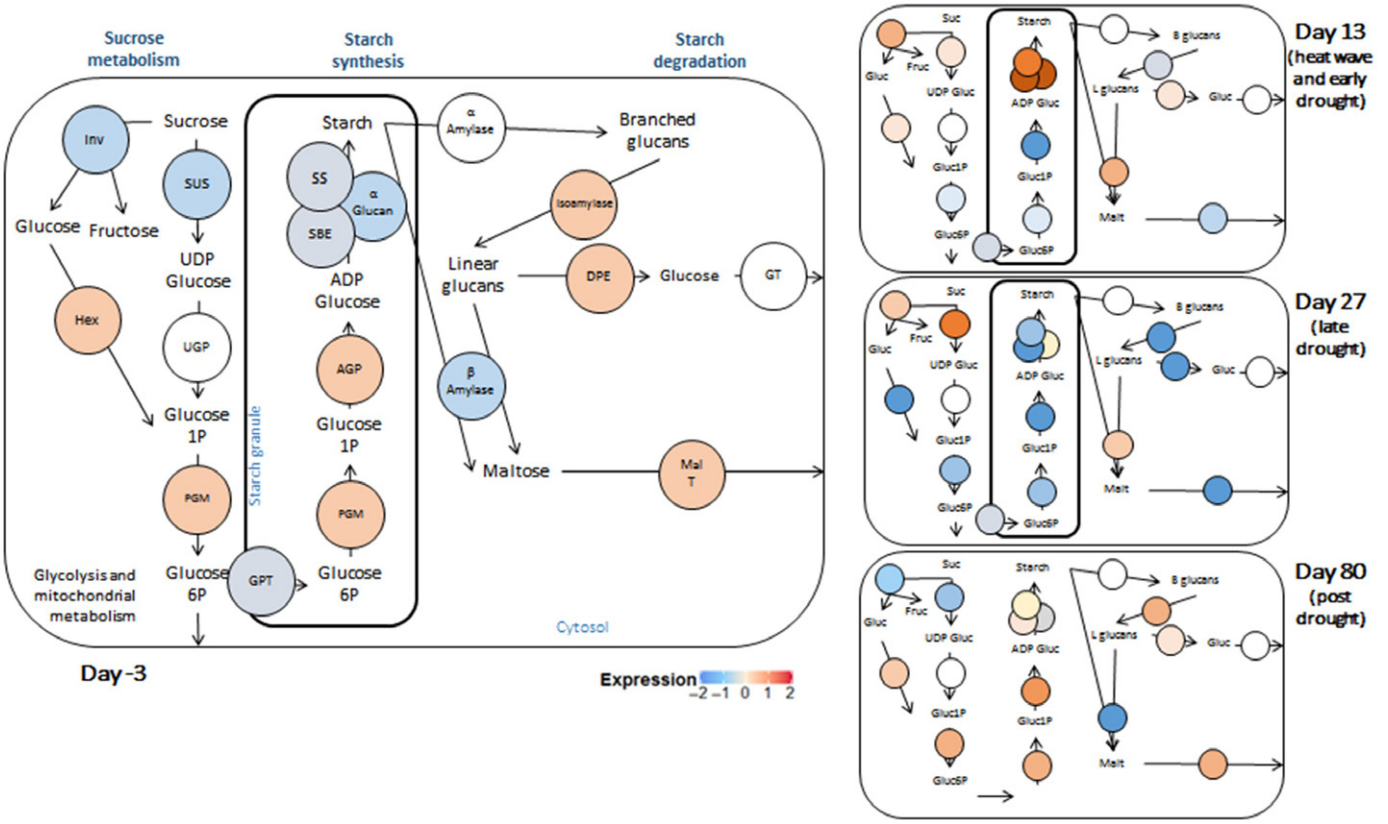

Fig. 10 Literature-based hypothesis of starch metabolism in wood, with observed enzyme expression dynamics under heat and drought. Circles denote enzymes. Colors represent upregulation/downregulation under specific scenarios. Suc, sucrose; Gluc, glucose; Fruc, fructose; Gluc1P, glucose-1-phosphate; Gluc6P, glucose-6-phosphate; B glucans, branched glucans; L glucans, linear glucans; Mal, maltose; SUS, sucrose synthase; UGP, UDP glucose pyrophosphorylase; PGM, phosphoglucomutase; AGP, ADP glucose pyrophosphorylase; SS, starch synthase; SBE, starch branching enzyme; DPE, disproportionating enzyme; Gluct, glucose transporter; Malt, maltose transporter.

The recovery response of dried trees, included induction of genes involved with starch synthesis (starch synthases 1, 4, 5, 8 and AGPs 1, 2 and 5) and degradation (starch phosphorylases 1, 2 and β amylases 1, 4, 6, 8 and 12). As mentioned, this response was not seen in watered trees. These genes are potentially related to the molecular management of the recovery process from drought, as presented in our third research question.

Identification of the gene family members related to mannitol and sucrose metabolism

Sucrose and mannitol concentrations increased during drought, a response particularly strong for mannitol. Polyol transporter genes were associated with mannitol fluctuations during drought. Out of three polyol transporters in this family, two were significantly upregulated while one was downregulated following drought, one of them highly correlated with mannitol content (Fig. 9). Polyol, mannitol, cinnamyl and 8-hydroxygeraniol transporters cannot be differentiated based on their amino acid sequence. A mannitol-specific transporter was studied in *O. europaea* cultured cells (Conde *et al.*, 2007, 2011), yet further evaluation is needed to define all mannitol transporters existing in the olive genome. Here we suggest Polyol transporter 2 (gene id: Oeu033162.1), which was upregulated significantly throughout drought in this experiment, as a mannitol transporter, regulated by plant environmental conditions.

Sucrose-related genes, converting sucrose to its components, potentially initiate many cellular functions, such as cell wall synthesis, mitochondrial metabolism and starch accumulation (Amor *et al.*, 1995; Fernie *et al.*, 2002). SUS and invertase, both catabolism genes involved in sucrose breakdown, are reported to be expressed in woody tissues of trees (Geisler-lee *et al.*, 2006; Lorenz *et al.*, 2011) and were highly expressed following abiotic stress in various species (Déjardin*et al.*, 1999; Kleines *et al.*, 1999; Dubos & Plomion, 2003; Lorenz *et al.*, 2011; Guerra *et al.*, 2015; Königshofer & Löppert, 2015; Fox *et al.*, 2018). Here, SUS and invertase genes have shown different expression patterns in drought, including upregulation throughout the drought period (SUS 1, invertases 2, 8 and 11) and some show downregulation in drought (SUSs 6, 7 and 11) (Fig. 6). Other sucrose-related genes were downregulated across the entire drought period (phosphoglucomutase 4) or in the end of drought (hexokinase 9) (Fig. 10). Therefore, there was an upregulation of genes involved with sucrose breakdown along with downregulation of genes involved with sucrose breakdown products. Together, these expression patterns were expected to cause an accumulation of sucrose breakdown products, glucose and fructose. This accumulation was not exhibited during drought. This discrepancy suggests the use of the degradation products in other pathways, such as mitochondrial metabolism. An additional explanation is the difference within branch tissues, which were not separated in this experiment and might host various processes, or unmeasured changes in enzymes level or activity.

Overall, the expression of starch metabolism enzymes, including sucrose metabolism, starch synthesis and degradation, and specific gene expression, imply elements of a complex mechanism containing various responses of transcripts, in turn related to heterogeneity in functions of each gene family.

Carbohydrate dynamics in woody tissues

Under drought, NSCs buffered the asynchrony between carbon supply, which decreased by 90%, and carbon demand, which had to maintain a minimum level for maintenance respiration. *Olea europaea* grows in the dry conditions of summer in the Mediterranean, when photosynthesis is limited, and hence must partly rely on stored NSCs. In our experiment, photosynthesis declined to *c.* $0\,\mu\mathrm{mol\,m^{-2}\,s^{-1}}$, as shown in other studies (Perez-Martin *et al.*, 2014). The measured water potential was lower than previously reported for olives (−6 MPa; Dichio *et al.*, 2009; Perez-Martin *et al.*, 2014), possibly reflecting the longer exposure to drought (28 d vs 13–15 d). In agreement with previous studies, starch, mannitol and sucrose were the most abundant components of NSCs in olive woody tissues (Drossopoulos & Niavis, 1988; Gómez-González *et al.*, 2010; Bustan *et al.*, 2011) while glucose and fructose were the lowest (Bustan *et al.*, 2011). The heat wave, which occurred during the first week, might have caused depletion in branch starch of all trees, with a stronger response in dried trees (starch percent in day 8 relative to baseline was 32% and 0% in watered and dried trees, respectively). Though starch reduction following soil drought alone (Mitchell *et al.*, 2013) and soil drought with high VPD (Drossopoulos & Niavis, 1988; Bustan *et al.*, 2011; Klein *et al.*, 2014) were previously shown, the separation between soil drought and VPD can indicate the proportional effect, perhaps via other processes such as photosynthesis, of these components to starch metabolism regulation. Starch depletion under water limitation, as a result of depleted photosynthesis, was also shown across species and tissues (Regier *et al.*, 2009; Mitchell *et al.*, 2013; Klein *et al.*, 2014; Lloret *et al.*, 2018). In addition, other storage compounds, that were reported in other trees species, might be used in olives such as lipids (Hoch *et al.*, 2003) and hemicellulose (Hoch, 2007). Mannitol increased in branches and roots together, making up 34% and 71% of total NSCs in branches on day 27 in watered and dried trees, respectively. Mannitol production may confer several potential advantages including a more efficient carbon use pathway, resistance to oxidative stress and use as an osmoprotectant (Stoop *et al.*, 1996; Jennings *et al.*, 1998). It is known as a significant soluble sugar of *O. europaea* in various tissues including leaves, fruits, branches and roots and a main photosynthetic product (Drossopoulos & Niavis, 1988; Stoop *et al.*, 1996; Dichio *et al.*, 2003; Gómez-González *et al.*, 2010; Lo Bianco & Scalisi, 2017). Leaves serve as a source and a storage tissue for mannitol (Flora & Madore, 1993; Conde *et al.*, 2008), and it tends to accumulate under abiotic stresses, such as drought and salinity (Tattini *et al.*, 1996; Probert *et al.*, 1998; Sofo *et al.*, 2007; Dichio *et al.*, 2009). Mannitol is synthesized from fructose as a precursor (Stoop *et al.*, 1996), while in this study fructose amounts were not high enough to explain mannitol accretion in branches. A possible explanation for mannitol accumulation is starch degradation into soluble sugars while fructose was rapidly used for mannitol. However, mannitol amounts presented in other publications of *O. europaea* leaves are consistent with mannitol accumulation demonstrated in this experiment. Hence, we assume mannitol was translocated from leaves and not produced in branches, as demonstrated in *Apium graveolens* (Davis & Loescher, 1990). In addition, the expression of the mannitol synthesis enzyme mannose 6-phosphate reductase, responsible for the exclusive stage in mannitol biosynthesis (Loescher *et al.*, 1992), was unchanged during drought (data not shown) while two polyol transporters were significantly highly expressed during water limitation (Fig. 8 in Conde *et al.*, 2011), suggesting translocation from other tissues.

NSCs and gene expression dynamics were measured from the same tissue, to ensure a valid comparison of results. However, closure of the carbon cycle within the trees, including their different tissues, was not performed in this study. Photosynthesis was measured in leaves while other measurements were conducted in branches and roots. Carbon allocation between the source tissue and the measured sink tissues was not evaluated. Another limitation was the use of a complex tissue, branches, while not separating it into its components (i.e. parenchyma, phloem, etc.). In order to better interpret some of our results, this separation is needed. In addition, studies in additional tree species will show the extent to which our results are generalizable. Nevertheless, we show that our integrated, though not exhaustive, approach is viable and opens the gate to future discoveries. The gene expression data from our experiment offers information on many additional pathways critical for tree drought and recovery adjustments, and is open for further exploration.

Our results demonstrate starch depletion following drought in branches prior to roots, while root NSCs of two trees out of six were high in the last day of drought (Fig. 3). Nondegradation of root starch at the same time as starch depletion in branches was previously shown in *Robinia pseudoacacia* (Zhang *et al.*, 2015). A prioritized degradation of starch in branches is proposed; suggesting two out of the six dried trees responded better to drought and did not exhaust their starch reserves yet. Taken together, our analysis proposes the first full starch metabolism pathway in woody tissues of trees during drought and recovery. This pathway should be further examined, to facilitate understanding of tree processes in a future of longer, hotter, droughts.

Acknowledgements

The authors are grateful to S. Wolf and N. Glanz (Hebrew University), for the HPLC analysis; to G. Ben-Ari (ARO Volcani Center) for sharing the database of the olive genome and for commenting on an earlier version of the manuscript, together with J. Gruenzweig (Hebrew University); and to the members of the Klein laboratory (Weizmann TreeLab) for helpful discussions and comments. Five anonymous referees are acknowledged for providing useful comments, which improved the article.

The authors thank the Merle S. Cahn Foundation; the Monroe and Marjorie Burk Fund for Alternative Energy Studies; Mr and Mrs Norman Reiser; the Weizmann Center for New Scientists; the estate of Helen Nichunsky; the Benoziyo Endowment Fund for the Advancement of Science; and the Edith & Nathan Goldberg Career Development Chair. MT is grateful for the support of the Women's League of Israel, with scholarships provided during her MSc research. The authors declare no competing interest in the preparation of this manuscript.

Author contributions

MT-R performed the study, which was initiated by TK. AS, YO-S and RD-S contributed to the design of the study. SB-D and EF assisted in the bioinformatic analysis. MT-R wrote the article, guided by TK and AS.

ORCID

Shifra Ben-Dor https://orcid.org/0000-0001-9604-1939
Rakefet David-Schwartz https://orcid.org/0000-0001-5923-8636
Tamir Klein https://orcid.org/0000-0002-3882-8845

Data availability

Data related to this research are reported in the text. GO annotations, complete gene sequences, and complete DESeq2 comparisons are provided in the Supporting Information Tables S1–S4, respectively.

References

Allen CD, Macalady AK, Chenchouni H, Bachelet D, McDowell N, Vennetier M, Kitzberger T, Rigling A, Breshears DD *et al.* 2010. A global overview of drought and heat-induced tree mortality reveals emerging climate change risks for forests. *Forest Ecology and Management* **259**: 660–684.

Amor Y, Haigler C h, Johnson S, Wainscott M, Delmer DP. 1995. A membrane-associated form of sucrose synthase and its potential role in synthesis of cellulose and callose in plants. *Proceedings of the National Academy of Sciences, USA* **92**: 9353–9357.

Angelopoulos K, Dichio B, Xiloyannis C. 1996. Inhibition of photosynthesis in olive trees (*Olea europaea* L.) during water stress and rewatering. *Journal of Experimental Botany* **47**: 1093–1100.

Bartlett MK, Klein T, Jansen S, Choat B, Sack L. 2016. The correlations and sequence of plant stomatal, hydraulic, and wilting responses to drought. *Proceedings of the National Academy of Sciences, USA* **113**: 13098–13103.

Bustan A, Avni A, Lavee S, Zipori I, Yeselson Y, Schaffer A, Riov J, Dag A. 2011. Role of carbohydrate reserves in yield production of intensively cultivated oil olive (*Olea europaea* L.) trees. *Tree Physiology* **31**: 519–530.

Chehab H, Mechri B, Mariem Fb, Hammami M, Ben Elhadj S, Braham M. 2009. Effect of different irrigation regimes on carbohydrate partitioning in leaves and wood of two table olive cultivars (*Olea europaea* L. cv. Meski and Picholine). *Agricultural Water Management* **96**: 293–298.

Conde A, Silva P, Agasse A, Conde C, Geros H. 2011. Mannitol transport and mannitol dehydrogenase activities are coordinated in *Olea Europaea* under salt and osmotic stresses. *Plant and Cell Physiology* **52**: 1766–1775.

Conde C, Silva P, Agasse A, Lemoine R, Delrot S, Tavares R, Geros H. 2007. Utilization and transport of mannitol in *Olea europaea* and implications for salt stress tolerance. *Plant and Cell Physiology* **48**: 42–53.

Conde C, Delrot S, Gerós H. 2008. Physiological, biochemical and molecular changes occurring during olive development and ripening. *Journal of Plant Physiology* **165**: 1545–1562.

Davis JM, Loescher WH. 1990. [14C]Assimilate translocation in the light and dark in celery (*Apium graveokns*) leaves of different ages. *Physiologia Plantarum* **79**: 656–662.

Déjardin A, Sokolov LN, Kleczkowski LA. 1999. Sugar/osmoticum levels modulate differential abscisic acid-independent expression of two stress-responsive sucrose synthase genes in Arabidopsis. *Biochemical Journal* **344**: 503–509.

Dichio B, Xiloyannis C, Angelopoulos K, Nuzzo V, Bufo SA, Celano G. 2003. Drought-induced variations of water relations parameters in *Olea europaea*. *Plant and Soil* **257**: 381–389.

Dichio B, Margiotta G, Xiloyannis C, Bufo SA, Sofo A, Cataldi TRI. 2009. Changes in water status and osmolyte contents in leaves and roots of olive plants (*Olea europaea* L.) subjected to water deficit. *Trees – Structure and Function* **23**: 247–256.

Dray S, Josse J. 2015. Principal component analysis with missing values: a comparative survey of methods. *Plant Ecology* **216**(5): 657–667.

Drossopoulos JB, Niavis CA. 1988. Seasonal changes of the metabolites in the leaves, bark and xylem tissues of olive tree (*Olea europaea.* L) II. Carbohydrates. *Annals of Botany* **62**: 321–327.

Dubos C, Plomion C. 2003. Identification of water-deficit responsive genes in maritime pine (*Pinus pinaster* Ait.) roots. *Plant Molecular Biology* **51**: 249–262.

Fernie AR. 2002. Sucrose to starch: a transition in molecular plant physiology. *Trends in Plant Science* **7**: 35–41.

Flora LL, Madore MA. 1993. Stachyose and mannitol transport in olive (*Olea europaea* L.). *Planta* **189**: 484–490.

Fox H, Doron-Faigenboim A, Kelly G, Bourstein R, Attia Z, Zhou J, Moshe Y, Moshelion M, David-Schwartz R. 2018. Transcriptome analysis of *Pinus halepensis* under drought stress and during recovery. *Tree Physiology* **38**: 423–441.

Fulton DC, Stettler M, Mettler T, Vaughan CK, Li J, Francisco P, Gil M, Reinhold H, Eicke S, Messerli G *et al.* 2008. β-Amylase4, a noncatalytic protein required for starch breakdown, acts upstream of three active β-amylases in Arabidopsis chloroplasts. *Plant Cell* **20**: 1040–1058.

Furze ME, Trumbore S, Hartmann H. 2018. Detours on the phloem sugar highway: stem carbon storage and remobilization. *Current Opinion in Plant Biology* **43**: 89–95.

Gambino G, Perrone I, Gribaudo I. 2008. A rapid and effective method for RNA extraction from different tissues of grapevine and other woody plants. *Phytochemical Analysis* **19**: 520–525.

Geisler-lee J, Geisler M, Coutinho PM, Segerman B, Nishikubo N, Takahashi J, Aspeborg H, Djerbi S, Master E, Andersson-Gunnerås S *et al.* 2006. Poplar carbohydrate-active enzymes. Gene identification and expression analyses. *Plant Physiology* **140**: 946–962.

Giorio P, Sorrentino G, d'Andria R. 1999. Stomatal behaviour, leaf water status and photosynthetic response in field-grown olive trees under water deficit. *Environmental and Experimental Botany* **42**: 95–104.

Gómez-González S, Ruiz-Jiménez J, Priego-Capote F, Luque de Castro MD. 2010. Qualitative and quantitative sugar profiling in olive fruits, leaves, and stems by gas chromatography-tandem mass spectrometry (GC-MS/MS) after ultrasound-assisted leaching. *Journal of Agricultural and Food Chemistry* **58**: 12292–12299.

Guerra D, Lamontanara A, Bagnaresi P, Orrù L, Rizza F, Zelasco S, Beghè D, Ganino T, Pagani D, Cattivelli L *et al.* 2015. Transcriptome changes associated with cold acclimation in leaves of olive tree (*Olea europaea* L.). *Tree Genetics and Genomes* **11**: 113.

Guindon S, Dufayard J-F, Lefort V, Anisimova M, Hordijk W, Gascuel O. 2010. New algorithms and methods to estimate maximum-likelihood phylogenies: assessing the performance of PhyML 3.0. *Systematic Biology* **59**: 307–321.

Gygi SP, Rochon Y, Franza BR, Aebersold R. 1999. Correlation between protein and mRNA abundance in yeast. *Molecular and Cellular Biology* **19**: 1720–1730.

Hartmann H, Trumbore S. 2016. Understanding the roles of nonstructural carbohydrates in forest trees – from what we can measure to what we want to know. *New Phytologist* **211**: 386–403.

Hoch G, Richter A, Korner Ch. 2003. Non-structural carbon compounds in temperate forest trees. *Plant, Cell & Environment* **26**: 1067–1081.

Hoch G. 2007. Cell wall hemicelluloses as mobile carbon stores in non-reproductive plant tissues. *Functional Ecology* **21**: 823–834.

Hummel I, Pantin F, Sulpice R, Piques M, Rolland G, Dauzat M, Christophe A, Pervent M, Bouteillé M, Stitt M *et al.* 2010. Arabidopsis plants acclimate to water deficit at low cost through changes of carbon usage: an integrated perspective using growth, metabolite, enzyme, and gene expression analysis. *Plant Physiology* **154**: 357–372.

Jennings DB, Ehrenshaft M, Pharr DM, Williamson JD. 1998. Roles for mannitol and mannitol dehydrogenase in active oxygen-mediated plant defense. *Proceedings of the National Academy of Sciences, USA* **95**: 15129–15133.

Kammerer B, Fischer K, Hilpert B, Schubert S, Gutensohn M, Weber A, Flügge U-I. 1998. Molecular characterization of a carbon transporter in plastids from heterotrophic tissues: the glucose 6-phosphate/phosphate antiporter. *Plant Cell* **10**: 105–117.

Kaplan F, Guy CL. 2004. Β-Amylase induction and the protective role of maltose during temperature shock. *Plant Physiology* **135**: 1674–1684.

Keel SG, Siegwolf R, Jäggi M, Körner C. 2007. Rapid mixing between old and new C pools in the canopy of mature forest trees. *Plant, Cell & Environment* **30**: 963–972.

Klein T, Hoch G, Yakir D, Korner C. 2014. Drought stress, growth and nonstructural carbohydrate dynamics of pine trees in a semi-arid forest. *Tree Physiology* **34**: 981–992.

Klein T, Vitasse Y, Hoch G. 2016. Coordination between growth, phenology and carbon storage in three coexisting deciduous tree species in a temperate forest. *Tree Physiology* **36**: 847–855.

Klein T, Hoch G. 2015. Tree carbon allocation dynamics determined using a carbon mass balance approach. *New Phytologist* **205**: 147–159.

Kleines M, Elster R-C, Rodrigo M-J, Blervacq A-S, Salamini F, Bartels D. 1999. Isolation and expression analysis of two stress-responsive sucrose-synthase genes from the resurrection plant *Craterostigma plantagineum* (Hochst.). *Planta* **209**: 13–24.

Kobe RK. 1997. Carbohydrate allocation to storage as a basis of interspecific variation in sapling survivorship and growth. *Oikos* **80**: 226.

Königshofer H, Löppert HG. 2015. Regulation of invertase activity in different root zones of wheat (*Triticum aestivum* L.) seedlings in the course of osmotic adjustment under water deficit conditions. *Journal of Plant Physiology* **183**: 130–137.

Landhäusser SM, Chow PS, Dickman LT, Furze ME, Kuhlman I, Schmid S, Wiesenbauer J, Wild B, Gleixner G, Hartmann H. 2018. Standardized protocols and procedures can precisely and accurately quantify non-structural carbohydrates. *Tree Physiology* **38**: 1764–1778.

Larkin MA, Blackshields G, Brown NP, Chenna R, McGettigan PA, McWilliam H, Valentin F, Wallace IM, Wilm A, Lopez R *et al.* 2007. Clustal W and Clustal X version 2.0. *Bioinformatics* **23**: 2947–2948.

Letunic I, Bork P. 2019. Interactive Tree of Life (iTOL) v4: recent updates and new developments. *Nucleic Acids Research* **47**: 256–259.

Lloret F, Sapes G, Rosas T, Galiano L, Saura-Mas S, Sala A, Martínez-Vilalta J. 2018. Non-structural carbohydrate dynamics associated with drought-induced die-off in woody species of a shrubland community. *Annals of Botany* **121**: 1383–1396.

Lo Bianco R, Scalisi A. 2017. Water relations and carbohydrate partitioning of four greenhouse-grown olive genotypes under long-term drought. *Trees – Structure and Function* **31**: 717–727.

Loescher WH, Tyson RH, Everard JD, Redgwell RJ, Bieleski RL. 1992. Mannitol synthesis in higher plants. *Plant Physiology* **98**: 1396–1402.

Lorenz WW, Alba R, Yu Y-S, Bordeaux JM, Simões M, Dean JFD. 2011. Microarray analysis and scale-free gene networks identify candidate regulators in drought-stressed roots of loblolly pine (*P. taeda* L.). *BMC Genomics* **12**: 264.

Loumou A, Giourga C. 2003. Olive groves: "The life and identity of the Mediterranean". *Agriculture and Human Values* **20**: 87–95.

Love MI, Huber W, Anders S. 2014. Moderated estimation of fold change and dispersion for RNA-seq data with DESeq2. *Genome Biology* **15**: 1–21.

Marchler-Bauer A, Lu S, Anderson JB, Chitsaz F, Derbyshire MK, DeWeese-Scott C, Fong JH, Geer LY, Geer RC, Gonzales NR *et al.* 2011. CDD: a conserved domain database for the functional annotation of proteins. *Nucleic Acids Research* **39**: 225–229.

Martínez-Vilalta J, Sala A, Asensio D, Galiano L, Hoch G, Palacio S, Piper FI, Lloret F *et al.* 2016. Dynamics of non-structural carbohydrates in terrestrial plants: a global synthesis. *Ecological Monographs* **86**: 495–516.

Mcdowell N, Pockman WT, Allen CD, Breshears DD, Cobb N, Kolb T, Plaut J, Sperry J, West A, Williams DG *et al.* 2008. Mechanisms of plant survival and mortality during drought: why do some plants survive while others succumb to drought? *New Phytologist* **178**: 719–739.

Mitchell PJ, O'Grady AP, Tissue DT, White DA, Ottenschlaeger ML, Pinkard EA. 2013. Drought response strategies define the relative contributions of hydraulic dysfunction and carbohydrate depletion during tree mortality. *New Phytologist* **197**: 862–872.

Monroe JD, Storm AR. 2018. Review: The Arabidopsis β-amylase (BAM) gene family: diversity of form and function. *Plant Science* **276**: 163–170.

Nogués S, Baker NR. 2000. Effects of drought on photosynthesis in Mediterranean plants grown under enhanced UV-B radiation. *Journal of Experimental Botany* **51**: 1309–1317.

Noronha H, Conde C, Delrot S, Gerós H. 2015. Identification and functional characterization of grapevine transporters that mediate glucose-6-phosphate uptake into plastids. *Planta* **242**: 909–920.

Noronha H, Silva A, Dai Z, Gallusci P, Rombolà AD, Delrot S, Gerós H. 2018. A molecular perspective on starch metabolism in woody tissues. *Planta* **248**: 559–568.

Pagliarani C, Casolo V, Ashofteh Beiragi M, Cavalletto S, Siciliano I, Schubert A, Gullino ML, Zwieniecki MA, Secchi F. 2019. Priming xylem for stress recovery depends on coordinated activity of sugar metabolic pathways and changes in xylem sap pH. *Plant, Cell & Environment* **42**: 1775–1787.

Perez-Martin A, Michelazzo C, Torres-Ruiz JM, Flexas J, Fernández JE, Sebastiani L, Diaz-Espejo A. 2014. Regulation of photosynthesis and stomatal and mesophyll conductance under water stress and recovery in olive trees: correlation with gene expression of carbonic anhydrase and aquaporins. *Journal of Experimental Botany* **65**: 3143–3156.

Probert ME, Carberry PS, McCown RL. 1998. Partitioning of photosynthetic carbohydrates in leaves of salt-stressed olive plants. *Australian Journal of Agricultural Research* **49**: 317–327.

Quentin AG, Pinkard EA, Ryan MG, Tissue DT, Baggett LS, Adams HD, Maillard P, Marchand J, Landhäusser SM, Lacointe A *et al.* 2015. Non-structural carbohydrates in woody plants compared among laboratories. *Tree Physiology* **35**: 1146–1165.

Regier N, Streb S, Cocozza C, Schaub M, Cherubini P, Zeeman SC, Frey B. 2009. Drought tolerance of two black poplar (*Populus nigra* L.) clones: contribution of carbohydrates and oxidative stress defence. *Plant, Cell & Environment* **32**: 1724–1736.

Rodriguez-Dominguez CM, Brodribb TJ. 2019. Declining root water transport drives stomatal closure in olive under moderate water stress. *New Phytologist* **225**: 126–134.

Ruiz-Peinado R, Montero G, del Rio M. 2012. Biomass models to estimate carbon stocks for hardwood tree species. *Forest Systems* **21**: 42–52.

Sala A, Woodruff D, Meinzer F. 2012. Carbon dynamics in trees: feast or famine? *Tree Physiology* **32**: 764–775.

Sauter JJ, van Cleve B. 1991. Biochemical and ultrastructural results during starch-sugar-conversion in ray parenchyma cells of Populus during cold adaptation. *Journal of Plant Physiology* **139**: 19–26.

Scholander PF, Bradstreet ED, Hemmingsen EA, Hammel HT. 1965. Sap pressure in vascular plants. *Science* **148**: 339–346.

Silpi U, Lacointe A, Kasempsap P, Thanysawanyangkura S, Chantuma P, Gohet E, Musigamart N, Clement A, Ameglio T, Thaler P. 2007. Carbohydrate reserves as a competing sink: evidence from tapping rubber trees. *Tree Physiology* **27**: 881–889.

Silva A, Noronha H, Dai Z, Delrot S, Gerós H. 2017. Low source–sink ratio reduces reserve starch in grapevine woody canes and modulates sugar transport and metabolism at transcriptional and enzyme activity levels. *Planta* 246: 525–535.

Smith AM, Zeeman SC, Smith SM. 2005. Starch degradation. *Annual Review of Plant Biology* 56: 73–98.

Smith AM. 2007. Starch biosynthesis and degradation in plants. *Encyclopedia of Life Sciences*. Hoboken, NJ: John Wiley & Sons doi: 10.1002/9780470015902.a0020124.

Sofo A, Manfreda S, Dichio B, Fiorentino M, Xiloyannis C. 2007. The olive tree: a paradigm for drought tolerance in Mediterranean climates. *Hydrology and Earth System Sciences Discussions* 4: 2811–2835.

Stoop J, Williamson J, Masonpharr D. 1996. Mannitol metabolism in plants: a method for coping with stress. *Trends in Plant Science* 1: 139–144.

Chapin FS, Schulze E, Mooney HA. 1990 The ecology and economics of storage in plants. *Annual Review of Ecology and Systematics* 21, 423–447.

Sulpice R, Pyl E-t, Ishihara H, Trenkamp S, Steinfath M, Witucka-Wall H, Gibon Y, Usadel B, Poree F, Piques MC. 2009. Starch as a major integrator in the regulation of plant growth. *Proceedings of the National Academy of Sciences, USA* 106: 10348–10353.

Tattini M, Gucci R, Romani A, Baldi A, Everard JD. 1996. Changes in non-structural carbohydrates in olive (*Olea europaea*) leaves during root zone salinity stress. *Physiologia Plantarum* 98: 117–124.

Thalmann M, Coiro M, Meier T, Thomas Wicker SC, Zeeman DS 2019. The evolution of functional complexity within the beta-amylase gene family in land plants. *BMC Evolutionary Biology* 19: 1–18.

Trumbore S, Czimczik CI, Sierra CA, Muhr J, Xu X. 2015. Non-structural carbon dynamics and allocation relate to growth rate and leaf habit in California oaks. *Tree Physiology* 35: 1206–1222.

Wiley E, Casper BB, Helliker BR. 2017. Recovery following defoliation involves shifts in allocation that favour storage and reproduction over radial growth in black oak. *Journal of Ecology* 105: 412–424.

Witt W, Sauter JJ. 1994. Starch metabolism in poplar wood ray cells during spring mobilization and summer deposition. *Physiologia Plantarum* 92: 9–16.

Xiloyannis C, Dichio B, Nuzzo V, Celano G. 1999. Defence strategies of olive against water stress. *Acta Horticulturae* 474: 423–426.

Zeeman SC, Kossmann J, Smith AM. 2010. Starch: its metabolism, evolution, and biotechnological modification in plants. *Annual Review of Plant Biology* 61: 209–234.

Zhang T, Cao Y, Chen Y, Liu G. 2015. Non-structural carbohydrate dynamics in *Robinia pseudoacacia* saplings under three levels of continuous drought stress. *Trees* 29: 1837–1849.

Zhou W, He S, Naconsie M, Ma Q, Zeeman SC, Gruissem W, Zhang P. 2017. Alpha-glucan, water dikinase 1 affects starch metabolism and storage root growth in Cassava (*Manihot esculenta Crantz*). *Scientific Reports* 7: 1–17.

Supporting Information

Additional Supporting Information may be found online in the Supporting Information section at the end of the article.

Fig. S1 Principle component analysis (PCA) of NSC variables in branches (starch, mannitol, sucrose, glucose and fructose percent) with physiological results (assimilation, transpiration and water potential) and plant conditions (VPD and SWC).

Fig. S2 Phylogenetic tree of the β amylase sequences.

Methods S1 Manual sequence curation and primer design; transcriptome assembly and differential expression; enrichment analysis; and construction of phylogenetic trees.

Notes S1 Transcriptomic changes in other carbon metabolism genes in olive under drought.

Table S1 Gene sequences.

Table S2 DESeq2 comparisons.

Table S3 GO annotations.

Table S4 Phylogenetic tree sequence information.